Optimal point of insertion and needle angle in neuraxial blockade using a midline approach

A study in Computed Tomography scans of adult patients

Vogt, Mark; Van Gerwen, Dennis J.; Lubbers, Wouter; Van Den Dobbelsteen, John J.; Hagenaars, Martin

Important note
To cite this publication, please use the final published version (if applicable).
Please check the document version above.

Optimal point of insertion and needle angle in neuraxial blockade using a midline approach: a study in computed tomography scans of adult patients.

Mark Vogt[1], Dennis J van Gerwen[2], Wouter Lubbers[3], John J van den Dobbelsteen[2], Martin Hagenaars[4].

[1]Department of Anesthesiology, Erasmus MC Sophia Children Hospital, Rotterdam, The Netherlands.

[2]Department of Biomechanical Engineering, Delft University of Technology, Delft, The Netherlands.

[3]Department of Anesthesiology, VU University Medical Center, Amsterdam, The Netherlands.

[4]Department of Anesthesiology, Canisius Wilhelmina Ziekenhuis, Nijmegen, The Netherlands.

Corresponding author:

Martin Hagenaars, MD, PhD, Department of Anesthesiology, Canisius Wilhelmina Ziekenhuis, Weg door Jonkerbos 100, 6532 SZ Nijmegen, The Netherlands.

Tel. +31243657721

Fax +31243657352

Email m.hagenaars@cwz.nl

Running head: Optimal insertion point neuraxial blockade.

1   Abstract.

2

3   Background and objectives:

4

5   Neuraxial blockade using a midline approach can be challenging. Part of this challenge lies in

6   finding the optimal approach of the needle to its target. The present study aimed at finding (1)

7   the optimal point of insertion of the needle between the tips of two adjacent spinous processes

8   and (2) the optimal angle relative to the skin at which the needle should approach the epidural or

9   subarachnoid space.

10

11   Methods:

12

13   A computer algorithm systematically analyzed computed tomography scans of vertebral

14   columns of a cohort of 52 patients. On midsagittal sections, the possible points of insertion of a

15   virtual needle and the corresponding angles through which the epidural or subarachnoid space

16   can be reached were calculated.

17

18   Results:

19

20   The point chosen to introduce the needle between two adjacent spinous processes determines the

21   range of angles through which the epidural or subarachnoid space can be reached. At the

22   thoracic interspaces 1-2 through 3-4, thoracic interspaces 5-6 through 9-10 and at the lumbar

23   vertebral interspaces 2-3 through 4-5, the optimal point of insertion is slightly *inferior to* the

24   point halfway between the tips of the spinous processes. For thoracic interspace 4-5, the optimal

25   point of insertion is slightly superior to the point halfway between the tips of the spinous

1 processes. For the other interspaces, the optimal point of insertion is approximately halfway

2 between the tips of the spinous processes. The optimal angle to direct the needle varies from 9

3 degrees at the thoracolumbar junction and at the lumbar interspaces 3-4 and 4-5, to 53 degrees

4 at the thoracic interspace 7-8.

5

6 Conclusions:

7

8 Our study has resulted in practical suggestions - based on accurate, reproducible measurements

9 in patients - as to where to insert the needle and how to angulate the needle when performing

10 neuraxial anesthesia using a midline approach.

11

1   Introduction.

2

3   Neuraxial blockade using a midline approach can be challenging. The number of attempts

4   should be kept as low as possible to reduce the chance of complications[1,2] and to optimize the

5   comfort of each patient. According to the literature, several factors may determine the difficulty

6   (eg defined as the number of attempts) of the intended puncture. Some factors are patient

7   related and beyond the influence of the clinician performing the procedure, including the age of

8   the patient and age-related degenerative changes,[3,4] body mass index,[3] deformities of the

9   spine,[5,6] the ability of the patient to flex his/her hips[6] and the palpability of bony landmarks.[5,6]

10   Other factors, however, can actually be influenced, such as the equipment used, the experience

11   of the clinician,[1,7] the positioning of the patient as chosen by the clinician,[3] and the point of

12   insertion of the needle. To the best of our knowledge, surprisingly few data exist on where

13   between the tips of the spinous processes the needle should be introduced and what the optimal

14   angle is to approach the subarachnoid or epidural space without bone contact. Data on this

15   subject would be very useful because choosing a point of insertion and angle is an unavoidable

16   step of this clinical procedure. For simplicity, in the subsequent text we mean both the

17   subarachnoid and the epidural space (ES), where only the ES is mentioned.

18   Previously, we demonstrated in a geometrical model that the point of insertion determines the

19   range of angles at which the ES can be reached.[8] Clinical data on this issue, however, are

20   difficult to find, and the scarce literature we found is not univocal.

21

22   For lumbar spinal anesthesia, it is suggested that the needle should be inserted either halfway

23   between the posterior spines [9], or closer to the superior spinous process [10], or closer to the

24   inferior spinous process.[11] We did not find research addressing the optimal insertion point for

25   thoracic epidural anesthesia.

1   Regarding the optimal angle to approach the ES, Pitkänen[12] suggests directing the needle at

2   10degrees when performing lumbar spinal anesthesia. For thoracic epidural anesthesia, we did

3   not find guidance regarding the best angle is to direct the needle. None of the afore mentioned

4   suggestions on how to perform neuraxial anesthesia using a midline approach are substantiated

5   by clinical research.

6   In order to establish a scientific rationale for choosing the optimal insertion point and insertion

7   angle during the actual clinical procedure, we studied the distribution of the optimal insertion

8   points and angles in real patients. We performed measurements in computed tomography-scans

9   of 52 patients at all different levels of the spine using a computer algorithm.

10

1   Methods.
2
3
4   Selection of CT scans.

5   The local ethical committee of the hospital (Canisius Wilhelmina Ziekenhuis, Nijmegen, The

6   Netherlands, investigation number 202-2013) gave consent to anonymously analyze CT scan

7   images for previously mentioned purposes. Only the sex and age of the patients were registered

8   (Table 1).

9   One of the radiologists at our hospital (Dr. L. Duijm) provided 52 CT-scans of a cohort of 52

10   adult patients. The CT scans of either the thorax, or the abdomen, or both were obtained for

11   various diagnostic purposes. No further selection criteria were applied.

12   One of the authors (MH) visually judged each CT-scan to assess whether analysis would be

13   feasible. A CT-scan was considered analyzable if a midsagittal cross-section provided a

14   complete, intact image of 2 adjacent spinous processes and the space between these processes, at

15   1 or more levels of the spine. For all 52 subjects, at each analyzable level, we determined the

16   optimal insertion point, and the optimal angle of insertion, as described in the following

17   sections.

18

19   Analysis of CT-scans.

20   *Determination of the levels of the vertebral interspaces.*

21   The level of a vertebral interspace was determined by verifying the location of the first rib

22   attached to the body of a vertebra in the CT scan. This vertebra represents Th1, the first thoracic

23   vertebral body. The levels of all other vertebral bodies (and thus the levels of the vertebral

24   interspaces) were determined by referring to Th1. In cases where the first rib and the

25   corresponding vertebra were not depicted, the sacrum was used as a reference.

26

27

1   *Numerical analysis of interspace geometry.*

2   A program was written in MATLAB R2015a (The Mathworks, Inc., Natick, Massachusetts) to

3   analyze the CT scans numerically, in an objective and reproducible manner. A detailed

4   explanation of the analysis method is available on request by email.

5   The CT scans were stored as JPG files. To prepare the CT scan data for analysis, the midsagittal

6   cross-sections of analyzable interspaces were segmented by manually delineating the boundaries

7   of the spinous processes (performed by MH), using a custom interface (Fig. 1, a and b). For

8   each interspace (Fig. 2a), a tangential reference line is drawn that connects the most dorsal

9   points of the 2 adjacent spinous processes that form a spinal interspace (Fig. 2b). We assume

10   that this tangent line is approximately parallel to the skin surface at this particular interspace.

11   The tangent line provides a well-defined reference for measuring the insertion points and angles.

12   To facilitate comparison between levels in 1 single subject and between different subjects, the

13   segmented spinous processes are rotated, translated, and scaled (Fig. 2c), so that, respectively,

14   the tangential line runs parallel to the (vertical) y-axis, the lowest point (A) on the tangential line

15   coincides with the origin of the axes system, and the distance between the extreme points (A and

16   B) on the tangential line is equal to one dimensionless unit.

17   We assume that the insertion point is located on the tangential line, that is, somewhere between

18   the extreme points A and B, such that its value ranges from 0 to 1. This range is subdivided into

19   1000 steps, and at each step, the smallest angle and the largest angle are determined at which the

20   ES can be reached without touching either of the spinous processes. Together, these two angles

21   determine the window size, θ, for that specific insertion point (Fig. 2d).

22   In total, 530 interspaces were considered analyzable according to the aforementioned criteria.

23   After having analyzed these 530 interspaces, we know all the possible combinations of insertion

24   points and insertion angles that allow access to the ES. We call these the *feasible approaches* to

25   the ES (an *approach,* in this context, is a combination of insertion point and angle).

1   We consider an *optimal* approach to be one that offers the best chance of successfully reaching

2   the ES in practice. To estimate the chance of success we need to consider the clinical context.

3

4

5   *Individual optimum versus generic optimum.*

6   Arguably, the best chance of success would be offered by planning the optimal approach for

7   each individual interspace with the help of imaging modalities such as CT, fluoroscopy or

8   ultrasound. If the interspace anatomy allows access to the ES, a perfectly executed individually

9   planned approach would always end in success, thus yielding a 100% success rate. However, the

10   actual success rate will be limited by the practitioner's ability to execute the planned approach.

11   For this reason, the *individual optimum* is defined here as the approach (insertion point and

12   angle) that maximizes the allowed margin of error for the practitioner.

13   On the other hand, if imaging modalities are not used or available (as is often the case), one has

14   to rely on experience in combination with guidelines, such as those described in the

15   introduction.[9-12] A guideline suggests a *generic* approach. Because of anatomic variability, a

16   generic approach cannot yield a 100% success rate, even if perfectly executed, but we can aim

17   for the best possible success rate. Thus, the *generic optimum* is defined here as the approach

18   (insertion point and angle) that maximizes the puncture success rate for a representative sample

19   of patients.

20   Both the individual optima and the generic optima are of practical interest. The methods used to

21   determine these optima for our dataset are described in the following sections.

22

23   *Determination of the individual optimum.*

24   Basic geometry tells us that the point of needle insertion directly determines the size of the

25   insertion window, that is, the range of angles at which the ES can be reached. We assume that

1 the larger this window, the larger the allowed margin of error, and the higher the probability of

2 successfully reaching the ES in 1 attempt.

3 Based on this premise, we define the optimal insertion point for a particular interspace to be that

4 point that maximizes the insertion window. Correspondingly, we define the optimal insertion

5 angle to be the angle in the center of this window, so as to allow an equal margin of error on

6 both sides, as depicted in Fig. 3a. The corresponding angle α is the angle between this line and a

7 line perpendicular to the line connecting A and B (dotted line, Fig. 3a).

8 The individual optima are collected from all subjects in our sample and are summarized as mean

9 values and their corresponding 95% confidence intervals (CIs) for each separate level of the

10 spine.

11

12 *Determination of the generic optimum.*

13 The generic optimum is that combination of insertion point and angle that would yield the

14 highest number of successful punctures when applied to all subjects in our sample. We define

15 the success rate as the number of successful punctures divided by the total number of punctures,

16 expressed as a percentage.

17 To determine the generic optimum for a specific vertebral level, we create a map of the success

18 rate (indicated in color scale) as a function of insertion point (y axis) and insertion angle (x

19 axis), as depicted in Fig. 5 for interspace L1-L2. To create this map, we divide the x-y plane into

20 a fine grid, each point on this grid representing a possible approach (insertion point and angle).

21 For each of these points, our algorithm then performs "virtual" punctures in all available L1-L2

22 interspaces in the dataset, and counts the number of punctures that successfully reach the ES.

23 This number is divided by the total number of punctures, to find the success rate.

1   This success map allows us to evaluate the theoretical success rate for any combination of

2   insertion point and insertion angle, and it allows us to easily locate those approaches that

3   provide the highest success rate (ie) the *generic* optima.

4   Success maps are available for all individual levels of the spine, for specific thoracic and lumbar

5   regions, and for the whole sample. The results of these success maps are numerically

6   summarized as median and corresponding interval.

7

1   Results.

2

3   *Patient population; sex and age.*

4   Computer tomography scans of 52 patients (32 females and 20 males) were analyzed. A

5   summary of the ages and sex of the patients is shown in Table 1. Of the studied population, 67%

6   is older than 60 years.

7

8   *Individual optima.*

9   Individual optima for all patients and all levels are presented in Fig. 4a, and a summary of these

10   data is provided in Table 2. Note that sample sizes vary because the imaged regions of the spine

11   differed between patients.

12   Fig. 4a shows that the mean optimal point of insertion is in general close to the center of the

13   spinous interspace. However, in the mid-thoracic and the lower-thoracic region (ie, Th5-Th6

14   through Th9-Th10), as well as in the lumbar region (L1-L2 through L4-L5), the mean optimal

15   point of insertion is slightly below the center of the spinous interspace. The variation in these

16   optimal points of insertion between individual subjects is considerable.

17   The optimal angle of insertion relative to the aforementioned tangential line is shown in Fig. 4b

18   and is summarized per level in Table 2. The mean optimal angle varies from 10degrees at the

19   interspace L2-L3 to 51degrees at the interspace Th6-Th7. The variation in these optimal angles

20   between individual subjects is considerable but is smaller than the variation in the optimal points

21   of insertion. Note that in some cases the optimal angle is negative.

22   The window sizes corresponding to the optimal points of insertion are shown in Fig. 4c. The

23   window size varies from 5degrees at the thoracic interspace Th5-Th6 and Th6-Th7 to 22degrees

24   at the thoracic level Th11-Th12 and at the thoracolumbar junction Th12-L1 . Again, the

25   variation between individual subjects is considerable. Note that the window sizes are at their

1   smallest when the spinous processes run the steepest, that is from Th5-Th6 through Th8-Th9.

2   Numerical data of the window sizes are shown in Table 2.

3   For all analyzed interspaces, we calculated the absolute distance in millimeters over the

4   tangential line where an insertion window was found, that is where it is possible to insert a

5   needle and reach the ES. The range of this distance varied from 8 mm (95% CI 6-10 mm) at

6   interspaces Th6-Th7, L3-L4 and L4-L5 to 17 mm (95% CI 15-18 mm) at Th11-Th12.

7   Plots of the interspace anatomy (with optimal insertion points, similar to Fig. 3a) are available

8   for all interspaces and all subjects as Supplemental Digital Content 1,

9   http://links.lww.com/AAP/A221.

10

11   *Generic optima.*

12   Using the known feasible approaches for all the 530 individual interspaces in our dataset, we

13   constructed maps of overall theoretical success rates for all individual levels of the spine. An

14   example is shown for interspace L1-L2 (Fig 5). The diagram shows the result for all possible

15   combinations of insertion angles (x-axis, ranging from -40 to 80 degrees) and insertion points (y

16   axis, ranging from 0 to 1, ie from point A to B, compare Fig. 2). The final result may be

17   compared with an altitude map. The maximal "altitude" (success rate, indicated in color scale) in

18   this diagram is 66% (21 out of 32) when combining an insertion angle of 11degrees (indicated

19   by the arrowhead on the x axis) with a insertion point of 0.5AB (indicated by the arrowhead on

20   the y axis). Similar maps were constructed for regions of the spine (high thoracic region, Th3-

21   Th6; low thoracic region, Th7-Th9; lumbar region, L2-L5) and for all accumulated data (Th1-

22   L5). The maps are available as Supplemental Digital Content 2,

23   http://links.lww.com/AAP/A222.

24   The distributions of the generic optima derived from these success maps are summarized in

25   Table 3. The results in this table may be interpreted as a practical guideline, indicating how to

1 puncture each separate level of the spine with the highest likelihood of reaching the ES in

2 attempt. For example, at the interspace L3-L4 our data indicate that insertion of the needle at

3 0.36AB with an angle of 9degrees results in a theoretical success rate of 32%. The maximum

4 achievable theoretical success rates for our sample range from 23% (7 of 31) at interspace Th5-

5 Th6 to 76% (35 of 46) at interspace Th11-Th12.

6

1 Discussion.

2

3 The anatomical boundaries of 530 spinous interspaces, derived from midsagittal CT sections of

4 52 patients, were analyzed numerically, in order to find all feasible approaches to the ES in

5 terms of needle insertion *point* and insertion *angle*. Based on all these feasible approaches, we

6 determined both the optimal *individual* approach for each available interspace, which maximizes

7 the allowed margin of error, and the optimal *generic* approach, which would give the highest

8 success rate when used as a rule-of-thumb for the whole sample. Success, in our context, was

9 defined as reaching the ES on the first attempt, without bone contact or needle redirections.

10

11 Our study provides insight into the anatomy of vertebral interspaces and their variability. To the

12 best of our knowledge, such information was not yet available in the literature. Forthcoming

13 from this anatomical analysis, our study clearly demonstrates that when using a midline

14 approach the range of angles at which the ES can be reached is dependent on the point of

15 insertion between the tips of the spinous processes. Many anesthesiologists perform both lumbar

16 and thoracic neuraxial blockade by a midline approach.[13] According to our measurements, the

17 available space for insertion to reach the ES varies on average from 8 to 17 mm. This suggests

18 that the proper selection of an insertion point for the needle tip is not only an academic exercise,

19 but also can indeed influence the chance of success.

20 In a previous study in a geometrical model[8], we found that the optimal point of insertion shifts

21 cranially when the spinous processes run steeper. We did not find this correlation in the CT

22 scans of real patients. The shape of the interspinous spaces was often such that a cranial point of

23 insertion does not allow an insertion window, in general because of bony spurs on the spinous

24 processes.

25

The *individual* optima presented in our study represent the ideal approach for each specific interspace in our sample. By definition, any of the *feasible* approaches identified for a specific interspace will yield a successful puncture in theory, but only the optimal approach maximizes the allowed margin of error for the practitioner. The methods used here to identify the individual optimum can be used in practice to plan an individualized approach based on imaging data. In addition, the individual optima, as presented in this study, give a good overall description of our dataset.

Especially important to note is the large variability between subjects within each level. This shows that a single *generic* approach will never be able to yield successful access to the ES in 100% of patients: not even if the generic approach is tailored to a specific vertebral level (based on many patients), and not even if the approach is always perfectly executed.

For example, the success-maps, as summarized in Table 3, show that the maximum achievable success rates when using a *generic* approach tailored to our sample range from 23% to 76%. These are theoretical upper limits: the only way to improve upon them is to use individualized planning or guidance methods.

The success maps from our study (eg Fig. 5) can be used to evaluate suggested approaches from the literature, simply by looking up the success rate corresponding to the suggested insertion point and/or angle. Most suggestions in the cited literature on how to perform lumbar neuraxial anesthesia when using a midline approach were not corroborated by our research, except the angle of 10degrees as suggested by Pitkänen.[12] The optimal puncture site for lumbar neuraxial blockade was found to be slightly *inferior* to the point halfway between the tips of the spinal processes and not – as suggested in the literature - closer to the superior spinous process[10], or halfway between the spinous processes[9] (except at level L1-L2) or closer to the inferior spinous process.[11]

1

2   We studied a patient cohort without further selection criteria. Patients of older age are more

3   represented in our sample. This might have biased our data.

4   We did not take the role of the positioning of the patient into account. The CT scans were made

5   for diagnostic purposes and not for the described research. In clinical practice for spinal and

6   epidural anesthesia, patients are either seated or put in the lateral recumbent position with their

7   chins on their chests, their shoulders lowered, and variable flexion of their hips. In contrast, the

8   patients presented in this study were lying on their backs without further adjustments of their

9   positioning. Previous research has shown the influence of the positioning of the patient on the

10   flexure of the spine and the degree of hip flexion[14] and therefore on the width between two

11   adjacent spinous processes.[16-19] Therefore, our results must be interpreted with caution. We

12   postulate that the optimal points of insertion of the needle may be studied more accurately in

13   optimally positioned subjects, ie in patients having their hips flexed.

14   On the other hand, the increase in width between adjacent spinous processes when increasing the

15   degree of hip flexion seems to be modest both in absolute and in relative numbers in the cited

16   studies. For example in the study by Fisher et al[15], the relative increase in width in the lumbar

17   interspaces was 1 mm or less in 60% (21 of 35 measurements) of the studied cases and 1 to 2

18   mm in 31%. The corresponding relative increases varied from 5 to 14% (≤1 mm) and from 12

19   to 33% (1 to 2 mm). In the study by Sandoval et al[17] (comparing the sitting position with

20   *un*supported feet to sitting with supported feet), the absolute increase of the width between 2

21   spinous processes was 1 mm or less in 9 of 16 cases; 1 to 2 mm in 4 of 16 cases; and more than

22   2 mm in 3 cases (being 2.1, 2.4, and 3.6 mm, respectively).

23   Furthermore, our study indicates that the shape of the *entire* space between 2 adjacent spinous

24   processes probably determines the accessibility of the ES and not only the width between two

25   arbitrarily chosen points. In addition, from clinical experience, we know that some patient

1   populations have difficulty flexing their hips, for example, elderly patients and pregnant

2   women.[19] Moreover, some studies suggest that the degree of hip flexion has only limited impact

3   on the difficulty to perform neuraxial anesthesia.[21-22]

4   Our calculations were performed without taking the dimensions of the needle into account and

5   under the assumption that the needle takes a straight course. From clinical experience and

6   experimental data we, know that this is not always the case[23].

7

8   We assume that many anesthesiologists, if not the majority, still perform neuraxial blockade

9   using the landmark-guided technique without additional aids. For these clinicians, an evidence-

10   based guideline tailored to a specific vertebral level may help improve the success rate. When

11   translating our data into practical guidelines one will encounter some difficulties. First , it is not

12   always possible to palpate the tips of the spinous processes, especially not in obese patients

13   having a lot of subcutaneous fat tissue on their backs. This means the insertion site will be

14   difficult to locate. Furthermore, it is difficult to accurately establish the exact level where the

15   puncture is performed[24], without the help of a reference point established, for example, by

16   imaging.

17   The next difficulty we envision is how to make an accurate estimation of the angle of the needle

18   relative to the skin under which the needle should approach the ES. One might use a sterile

19   protractor, as was done in the study by Helayel et al[25].

20   To maximize puncture success rates, we hypothesize that some form of imaging support is

21   necessary.

22

23   The ultrasound –guided technique is increasingly used for neuraxial blockade.[26] In this context,

24   the study by Helayel et al[25] is of interest. They performed lumbar epidural anesthesia for

25   various surgical interventions. Before performing the puncture, they measured the distance from

1   the skin to the ES by ultrasound after optimizing the obtained image. This site was marked and

2   subsequently used as puncture site for the needle. The angle of the transducer was measured

3   using a protractor. The epidural needle was inserted at an identical angle. This method was

4   apparently very effective, since only 1 skin puncture was needed in all subjects (n=60) and in

5   45% of the cases, redirection of the needle was necessary. Helayel et al[25] found no correlation

6   between the need to reposition the needle after insertion and the difference they found between

7   the 2 angles (measured at the transducer and at the needle with a protractor). This might suggest

8   that the optimal obtained image by ultrasound resembles the optimal point of insertion as we

9   defined in our study.

10

11 Fluoroscopy has also been suggested to improve success rates of epidural puncture. In a recent

12 study, it was shown that fluoroscopic guidance did increase the incidence of correct placement

13 of a catheter in the thoracic epidural space compared with conventional loss of resistance

14 technique.[27] This increase was correlated with shorter post anesthesia care unit and hospital

15 lengths of stay. It was not correlated with differences in 24-hour opioid consumption or numeric

16 pain scores. The study does not give information regarding the ease of performance of epidural

17 puncture when using fluoroscopy.

18

19 In summary, our research has resulted in a practical strategy as to how epidural or spinal

20 anesthesia may be performed when using a midline approach. At all levels of the vertebral

21 column where neuraxial blockade is common practice, our calculations suggest (albeit with

22 considerable inter-individual variation) an optimal point of insertion of the needle between the

23 spinous processes and an optimal angle for directing the needle relative to the overlying skin.

24 To the best of our knowledge, this is the first time that practical suggestions for performing a

25 puncture for neuraxial blockade in the midline are substantiated by accurate and reproducible

1   measurements in patients. We hypothesize that our data – when interpreted cautiously - may

2   improve clinical performance for anesthesiologists using the landmark-guided method. To

3   maximize success rates, clinical aids such as ultrasound or fluoroscopy will probably be

4   required, although the benefits of these techniques have been contested.[27] Further research is

5   needed to establish if these proposed refinements in clinical practice result in higher success

6   rates and if they can reduce the chance of complications and increase patient comfort.

7

8

14

References.

1. De Oliveira Filho GR, Gomes HP, da Fonseca MHZ, Hoffman JC, Pederneiras SG, Garcia JHS. Predictors of successful neuraxial block: a prospective study. *Eur J Anaesthesiol* 2002;19(6):447-451.

2. Kang XH, Bao FP, Xiong XX, Li M, Jin TT, Shao J, Zhu SM. Major complications of epidural anesthesia: a prospective study of 5083 cases at a single hospital. *Acta Anaesthesiol Scand* 2014;58(7):858-866.

3. Ruzman T, Gulam D, Harsanji I, Drenjancevic, Venzera-Azenic D, Ruzman N, Burazin J. Factors associated with difficult neuraxial blockade. *Local Reg Anesth* 2014;7:47-52.

4. Tessler MJ, Kardash K, Wahba RM, Kleiman SJ, Trihas ST, Rossignol M. The performance of spinal anesthesia is marginally more difficult in the elderly. *Reg Anesth and Pain Med* 1999;24(2):126-130.

5. Atallah MM, Demian AD, Shorrab AA. Development of a difficulty score for spinal anaesthesia. *Br J Anaesth* 2004;92(3):354-360.

6. Guglielminotti J, Mentré F, Bedairia E, Montraves P, Lamgrois D. Development and evaluation of a score to predict difficult epidural placement during labor. *Reg Anesth Pain Med* 2013;38 (3):233-238.

7. Kim JH, Song SY, Kim BJ. Predicting the difficulty in performing a neuraxial blockade. *Korean J Anesthesiol* 2011;61(5):377-381.

8. Vogt M, van Gerwen DJ, van den Dobbelsteen JJ, Hagenaars M. Optimal point of insertion of the needle in neuraxial blockade using a midline approach: study in a geometrical model. *Local Reg Anesth* 2016;9:39-44.

9. Fettes, PDW, Jansson J-R, Wildsmith JA. Failed spinal anaesthesia: mechanisms, management, and prevention. *Br J Anaesth* 2009;102(6):739-748.

10. Veering BT, Cousins MJ. Epidural Neural Blockade. In: Cousins MJ, Carr DB, Horlocker TT, Bridenbaugh PO. *Cousin's & Bridenbaugh's Neural Blockade in Clinical Anesthesia and Pain Medicine*. 4th ed.Philadelphia, PA: Lippincott Williams & Wilkins, 2009.

11. Boon JM, Abrahams PH, Meiring JH, Welch T. Lumbar puncture: anatomical review of a clinical skill. *Clin Anat* 2004;17(6):544-553.

12. Pitkänen M. Spinal (Subarachnoid) blockade. In: Cousins MJ, Carr DB, Horlocker TT, Bridenbaugh PO. *Cousin's & Bridenbaugh's Neural Blockade in Clinical Anesthesia and Pain Medicine*. 4th ed. Philadelphia, PA: Lippincott Williams & Wilkins, 2009.

13. Wantman A, Hancox N, Howell PR. Techniques for identifying the epidural space: a survey of practice amongst anaesthetists in the UK. *Anaesthesia* 2006;61(4):370-375.

14. Stokes IAF, Abery JM. Influence of the hamstring muscles on lumbar spine curvature in sitting. *Spine* 1980;5(6):525-528.

15. Fisher A, Lupu L, Gurevitz B, Brill S, Margolin E, Hertzanu Y. Hip flexion and lumbar puncture: a radiological study *Anaesthesia* 2001;56(3):262-266.

16. Capogna G, Celleno D, Simonetti C, Lupoi D. Anatomy of the lumbar epidural region using magnetic resonance imaging: a study of dimensions and a comparison of two postures. *Int J Obstet Anesth* 1997;6(2):97-100.

17. Sandoval M, Shestak W, Stürmann K, Hsu C. Optimal patient positioning for lumbar puncture, measured by ultrasonography. *Emerg Radiol* 2004;10(4):179-181.

18. Abo A, Chen L, Johnston P, Santucci K. Positioning for lumbar puncture in children evaluated by bedside ultrasound. *Pediatrics* 2010;125(5):e1149-1153.

19. Ellinas EH, Eastwood DC, Patel SN, Maitra-D'Cruze AM, Ebert TJ. The effect of obesity on neuraxial technique difficulty in pregnant patients: a prospective, observational study. *Anesth Analg* 2009;109(4):1225-1231.

20. Fisher KS, Arnholt AT, Douglas ME, Vandiver SL, Nguyen DH. A randomized trial of the traditional sitting position versus the hamstring stretch position for labor epidural needle placement. *Anesth Analg* 2009;109(2):532-534.

21. Biswas BK, Agarwal B, Bhattarai B, Dey S, Bhattacharyya P. Straight versus flex back: does it matter in spinal anaesthesia? *Indian J Anaesth* 2012;56(3):259-264.

22. Soltani Mohammadi S, Hassani M, Marashi SM. Comparing the squatting position and traditional sitting position for ease of spinal needle placement: a randomized clinical trial. *Anaesth Pain Med* 2014;4(2):e13969.

23. Özdemir HH, Demir CF, Varol S, Arslan D, Yildiz M, Akil E. The effects of needle deformation during lumbar puncture. *J Neurosci Rural Pract* 2015;6(2):198-201.

24. Lirk P, Messner H, Deibl M, Mitterschiffthaler G, Colvin J, Steger B, Rieder J, Keller C. Accuracy in estimating the correct intervertebral space level during lumbar, thoracic and cervical epidural anaesthesia. *Acta Anaesthesiol Scand* 2004;48(3):347-349.

25. Helayel PE, da Conceição DB, Meurer G, Swarovsky C, de Oliveira Filho, GR. Evaluating the depth of the epidural space with the use of ultrasound. *Rev Bras Anestesiol* 2010;60(4):376-382.

26. Chin KJ, Karmakar MK, Peng PP. Ultrasonography of the adult thoracic and lumbar spine for central neuraxial blockade. *Anesthesiology* 2011;114(6):1459-1485.

27. Parra MC, Washburn K, Brown JR, Beach ML, Yeager MP, Barr P, Bonham K, Lamb K, Loftus RW. Fluoroscopic guidance increases the incidence of thoracic

epidural catheter placement within the epidural space: a randomized trial. *Reg Anesth Pain Med* 2017;42(1):17-24.

Table 1.

Computed tomography scans of 52 patients (32 females and 20 males) analyzed according to age. A summary of the ages and sex of the patients is shown. Sixty-seven percent of the studied population is 61 years or older.

Age (years)	Male (number)	Female (number)	Total (number)
0-30	0	1	1
31-40	1	4	5
41-50	3	2	5
51-60	4	2	6
61-70	4	12	16
71-80	6	7	13
>80	4	2	6
Total (number)	22	30	52

Table 2.

Summarized numerical data of the analysis of computer tomography scans of 52 patients.
For each level of the vertebral column (interspace name, first column) the sample size
(second column) and the optimal point of insertion of the needle (third column) with the
corresponding 95% CI are shown. In the fifth and seventh columns, for each level of the
vertebral column, the optimal angle and the window size (in degrees, with the corresponding
95% CI) are shown. The optimal point of insertion of the needle is at most vertebral
interspaces approximately halfway between the tips of the spinous processes. At the thoracic
levels Th6-Th7 through Th9-Th10 and at the lumbar levels L1-L2 through L4-L5, the optimal
point of insertion is in general slightly inferior to the point halfway between the tips of the
spinous processes. The mean optimal angle for insertion of the needle varies from 10 degrees
at interspace L2-L3 to 51 degrees at interspace Th6-Th7. The window size varies from 5
degrees at the thoracic levels Th5-Th6 and Th6-Th7 to 22 degrees at the thoracic level Th11-
Th12 and at the thoracolumbar junction Th12-L1.

interspace name	sample size [-]	location [-]		angle [deg]		window size [deg]		useful interspace height [mm]	
		mean	95%-CI	mean	95%-CI	mean	95%-CI	mean	95%-CI
Th1-Th2	20	0.59	(0.51, 0.66)	22	(18, 27)	9	(7, 11)	15	(13, 18)
Th2-Th3	27	0.53	(0.45, 0.61)	27	(24, 30)	8	(7, 9)	14	(12, 16)
Th3-Th4	31	0.52	(0.46, 0.59)	31	(27, 34)	7	(6, 8)	13	(11, 15)
Th4-Th5	30	0.59	(0.53, 0.65)	35	(32, 39)	7	(5, 8)	13	(11, 16)
Th5-Th6	27	0.48	(0.41, 0.55)	48	(43, 52)	5	(4, 7)	10	(8, 12)
Th6-Th7	28	0.34	(0.26, 0.42)	51	(47, 55)	5	(4, 7)	8	(6, 10)
Th7-Th8	31	0.36	(0.29, 0.43)	49	(46, 52)	7	(5, 8)	9	(7, 11)
Th8-Th9	35	0.45	(0.38, 0.52)	41	(37, 44)	8	(7, 10)	11	(9, 12)
Th9-Th10	35	0.45	(0.38, 0.51)	31	(28, 35)	10	(8, 11)	9	(8, 11)
Th10-Th11	42	0.53	(0.48, 0.58)	21	(17, 24)	14	(12, 15)	13	(12, 15)
Th11-Th12	46	0.53	(0.50, 0.57)	14	(12, 15)	22	(20, 25)	17	(15, 18)
Th12-L1	41	0.53	(0.48, 0.57)	12	(10, 14)	22	(19, 24)	16	(13, 18)
L1-L2	32	0.47	(0.42, 0.51)	13	(11, 15)	20	(16, 24)	13	(11, 16)
L2-L3	29	0.43	(0.38, 0.49)	10	(8, 13)	14	(10, 18)	10	(8, 12)
L3-L4	25	0.36	(0.31, 0.41)	11	(7, 14)	12	(9, 15)	8	(7, 10)
L4-L5	23	0.29	(0.24, 0.34)	13	(9, 17)	10	(7, 12)	8	(6, 10)

Table 3.

Summarized numerical data of the calculated success rates for all 530 analyzed interspaces (Th1-L5), for regions of the spine (eg Th3-Th6) and for individual levels of the spine (from Th1-Th2 to L4-L5) . For each specified level, the optimal combination of insertion point and insertion angle is indicated that will result in the highest success rate. This table may be viewed as a guideline how to perform neuraxial blockade at different levels of the spine. For example, when inserting a needle at lumbar level L3-L4 at 0.36AB and at 9^0, this will theoretically lead to a success rate of 32% in our sample.

#	level(s)	sample size	max. success	insertion point		angle	
				median	interval	median	interval
[-]	[-]	[-]	[%]	[-]	[-]	[deg]	[deg]
1	Th1-L5	530	24	0.47	-	21	-
2	Th3-Th6	93	19	0.54	[0.52,0.56]	39	[37,40]
3	Th7-Th9	71	31	0.28	[0.28,0.28]	49	[49,49]
4	L2-L5	82	35	0.40	[0.39,0.41]	7	[6,7]
5	Th1-Th2	20	40	0.35	[0.25,0.57]	29	[17,33]
6	Th2-Th3	28	36	0.40	[0.28,0.57]	34	[26,38]
7	Th3-Th4	31	32	0.39	-	33	-
8	Th4-Th5	31	26	0.67	[0.66,0.69]	31	[30,32]
9	Th5-Th6	31	23	0.36	-	52	-
10	Th6-Th7	33	24	0.30	[0.29,0.32]	46	[46,47]
11	Th7-Th8	34	29	0.22	-	53	-
12	Th8-Th9	37	43	0.28	[0.27,0.29]	49	[48,49]
13	Th9-Th10	38	42	0.47	[0.46,0.47]	33	[33,33]
14	Th10-Th11	45	53	0.54	[0.50,0.65]	21	[15,22]
15	Th11-Th12	46	76	0.56	-	14	-
16	Th12-L1	42	74	0.60	[0.59,0.61]	9	[8,10]
17	L1-L2	32	66	0.50	[0.48,0.52]	11	[10,13]
18	L2-L3	29	48	0.43	[0.40,0.53]	12	[2,15]
19	L3-L4	28	32	0.36	[0.30,0.48]	9	[2,21]
20	L4-L5	25	44	0.34	[0.33,0.34]	9	[8,11]
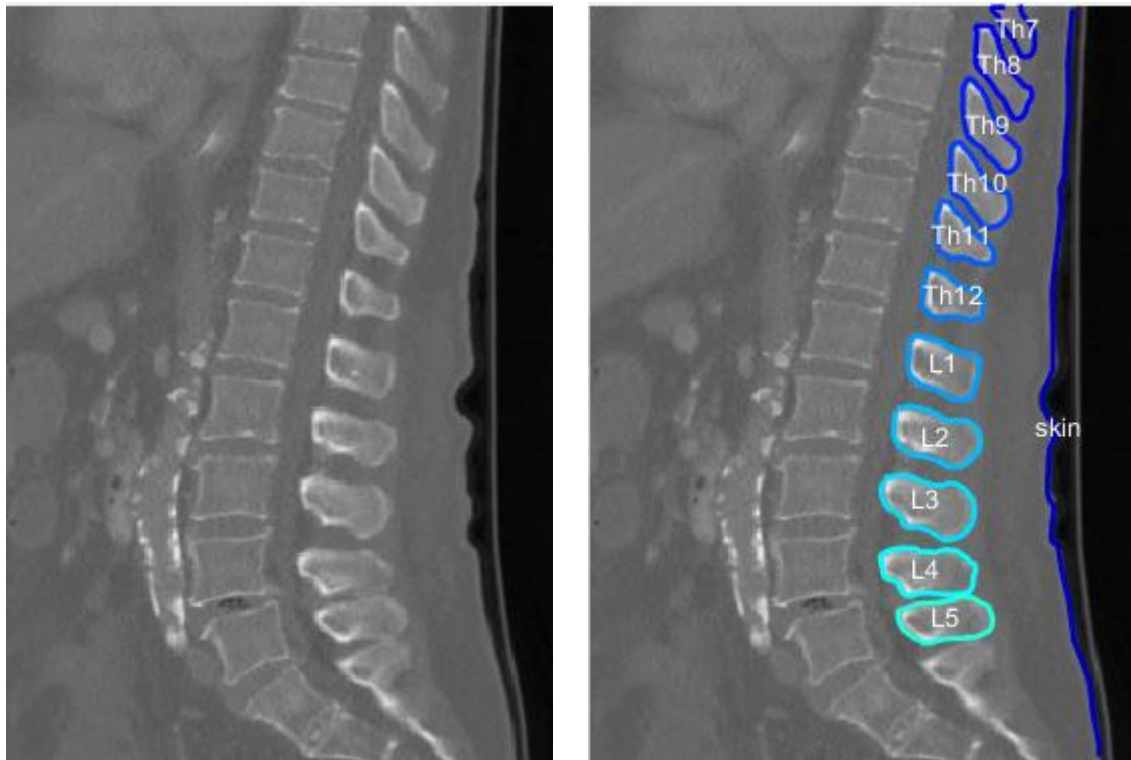
A   B

Figure 1.

A CT scan of a patient showing a midsagittal cross section of the vertebral column (A). At all

levels in the CT scan, the spinal interspaces and the upper and lower spinous processes are

virtually completely depicted. Therefore, all these levels are considered analyzable. For this

purpose, the circumferences of all spinous processes are delineated with the help of a

program written in MATLAB (B). By capturing the circumferences of the spinous processes

delineating the spinous interspaces, accurate and reproducible calculations were feasible to

obtain the optimal point of insertion and the optimal angle relative to the skin of a virtual
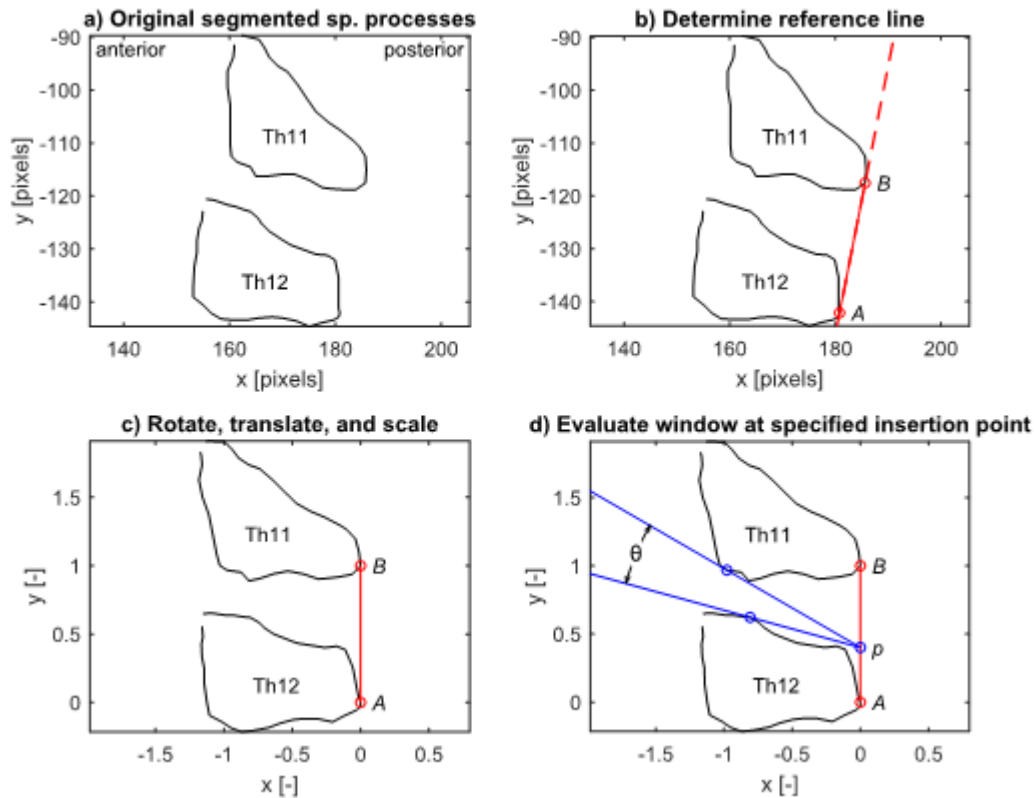
needle at each interspace.

Figure 2.

Example of an interspace being analyzed for the optimal point of insertion (A). A tangential

reference line is calculated connecting the most dorsal points of the 2 adjacent spinous

processes that formed a spinal interspace (B). The tangential line is subsequently rotated

together with the circumferences of the spinous processes, such that the tangential line runs

parallel to the y axis. The distance between the extreme points on the tangential line is

normalized to 1 (arbitrary units) to facilitate comparisons between levels in 1 single patient

and between patients (C). Subsequently, for each separate possible point of insertion on the

line connecting point A and B, it is calculated whether the ES can be attained and if so how

large the insertion window size is. An example is shown in D. Here, for a possible point of

insertion p of a virtual needle, the corresponding insertion window - represented by θ - is

depicted. For each analyzable interspace of each patient, the insertion point (running variable

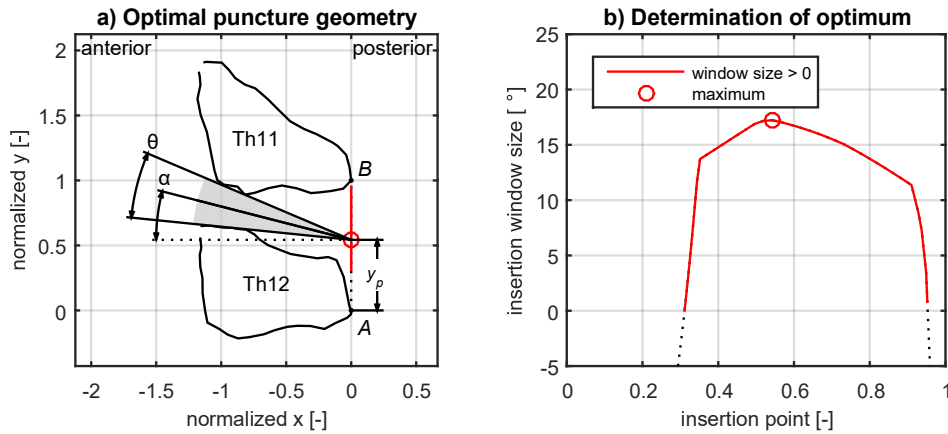on the x axis) is plotted against the insertion window (y axis).

Figure 3.

Example of an analyzable thoracic interspace Th11-Th12 of an arbitrarily chosen patient (A). The range of the calculated points of insertion of a virtual needle is indicated on the y axis (from 0 to 1 in arbitrary units). An example of an optimal point of insertion is depicted by the open red circle (A, corresponding with the open red circle in the diagram on the right, B). The insertion window (θ degrees) is indicated by the shaded area. The optimal angle to approach the ES is in the center of the shaded area, represented by the black line (A). The corresponding angle α is the angle between this line and a line perpendicular to the line connecting A and B (dotted line). The corresponding plot of the point of insertion (running variable on the x axis) against the insertion window (y axis) is shown in the diagram on the right (B).

a) Optimal insertion point

b) Optimal insertion angle
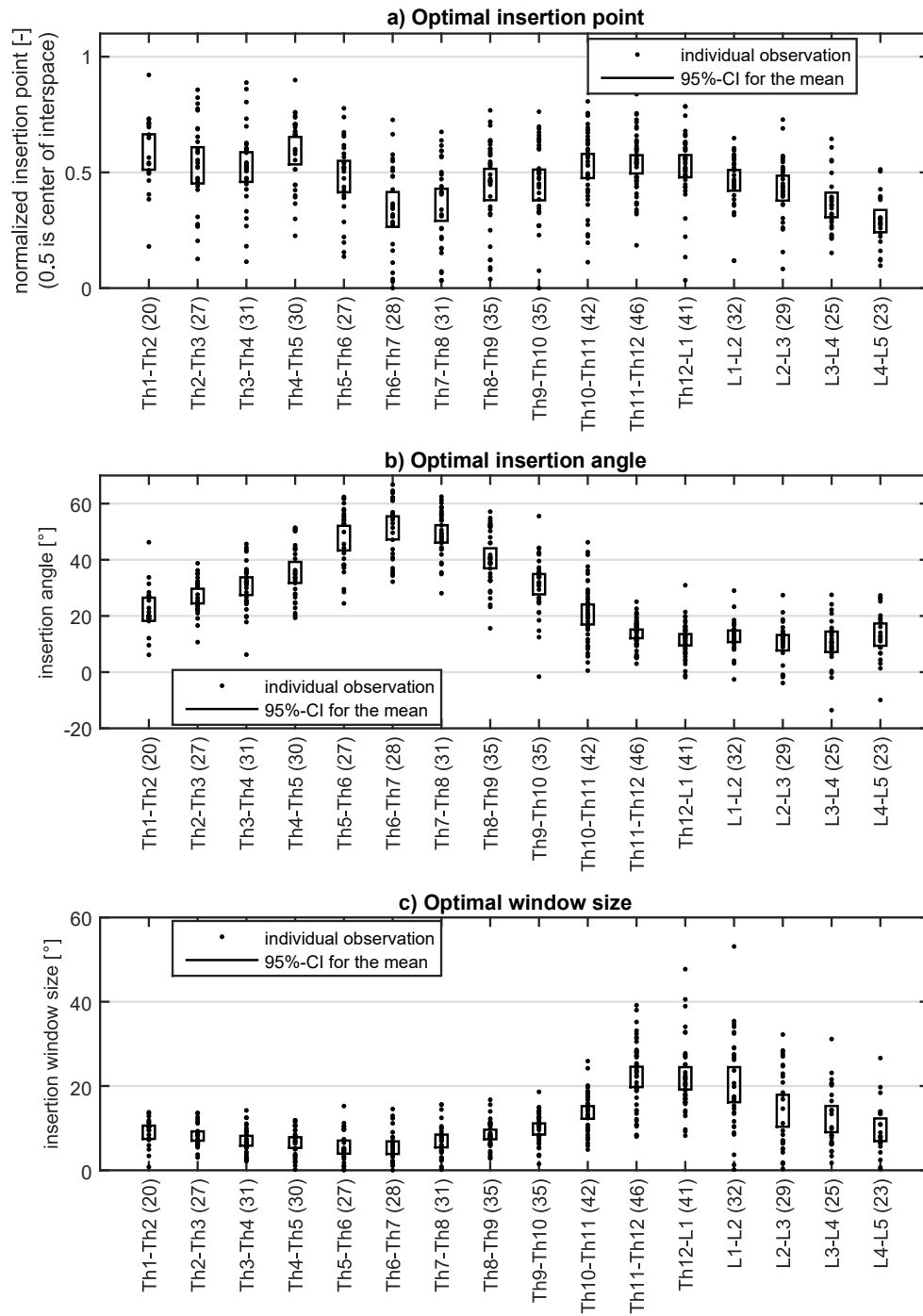
c) Optimal window size

Figure 4.

A, The vertebral interspace (x axis) is plotted against the normalized optimal point of insertion (y axis). Each dot represents the optimal point of insertion at the indicated interspace of 1 single patient. The box indicates the 95% CI at each interspace level. The sample size at each interspace is indicated in parentheses. In the midthoracic and the low thoracic region (ie, Th5-Th6 through Th9-Th10), as well as in the lumbar region (ie, L1-L2 through L4-L5), the optimal point of insertion is generally slightly inferior to the center of the interspace. For most of the other levels of the vertebral column, the optimal point of insertion is in general close to the center of the spinous interspace. The variation between individuals of these optimal points of insertion is large.

B, The vertebral interspace (x axis) is plotted against the insertion angle in degrees (y axis). Each dot represents the optimal angle of insertion at the indicated interspace of one single patient. The box indicates the 95% CI at each interspace level. The sample size at each interspace is indicated in parentheses (x axis). The mean optimal angle varies from 10degrees at the lumbar interspace L2-L3 to 51degrees at the thoracic interspace Th6-Th7.

C, The vertebral interspace (x axis) is plotted against the insertion window size in degrees (y axis). Each dot represents the window size corresponding with the optimal point of insertion at the indicated level of the vertebral column, in each individual patient. The box indicates the 95% CI at each interspace level. The sample size at each interspace is indicated in parentheses. The mean window size varies from 5degrees at Th5-Th6 and Th6-Th7 to 22degrees at Th11-Th12 and Th12-L1.
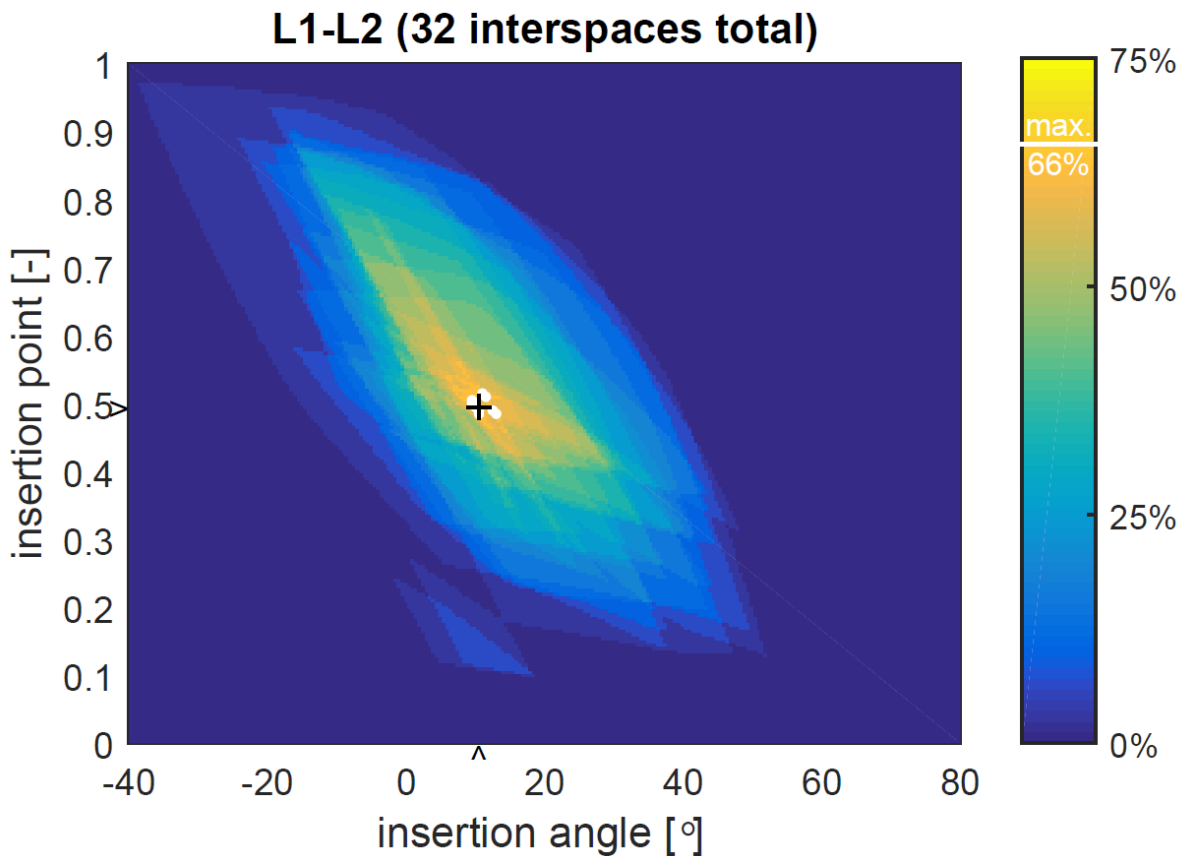
Figure 5.

The accumulated data of all 32 analyzed interspaces L1-L2 are shown. The insertion angle is

indicated on the x axis (in degrees) and the insertion point is indicated on the y axis (arbitrary

units). One single point in the diagram shows a combination of a chosen insertion point and

angle. For each combination, it is calculated if it will result in success, ie if the ES is reached

without bone contact. By adding all successful attempts and dividing this number by the total

number of attempts, a success percentage is calculated for this specific combination of

insertion point and angle. The entire diagram shows the result for all possible combinations

of insertion angles (ranging from -40 to 80 degrees) and insertion points (ranging from point

A to B, i.e. from 0 to 1 (arbitrary units), compare Fig. 2). The final result may be compared

with an altitude map. The maximal "altitude" (success rate) in this diagram is 66% (21 of 32)

when combining an insertion angle of 11degrees (indicated by the arrowhead on the x axis)

with a insertion point of 0.5AB (indicated by the arrowhead on the y axis). This maximal

success rate is indicated in white in the diagram. This white area represents a small set of combinations of insertion angles and insertion points with minimal differences in the resulting success rate. The median value of the success rates of these combinations in the white area is indicated by the plus sign (+).

Explanation of the diagrams in the Supplemental Digital Content, showing the puncture success rates per region.

The first diagram shows all the combinations of insertion angles (x-axis) and insertion points (y-axis) of a single patient on a single vertebral level, i.e. Th11-Th12. So any combination of insertion point and angle within the yellow area (indicating 100% success, see color scale) will result in access to the ES.

The next diagram shows the accumulated data of all analyzed interspaces (530 interspaces in total). The insertion angle is indicated on the x-axis (in degrees) and the insertion point is indicated on the y-axis (arbitrary units). One single point in the diagram shows a combination of a chosen insertion point and angle. For each interspace, it is calculated if this specific combination of insertion point and angle will result in success, i.e. if the ES is reached without bone contact. By adding all successful attempts and dividing this number by the total number of attempts, a success percentage is calculated for this specific combination of insertion point and angle. The entire diagram shows the result for all possible combinations of insertion angles (ranging from -40^0 to 80^0) and insertion points (ranging from 0 to 1, i.e. from point A to B, compare Figure 2). The final result may be compared with an altitude map. The maximal "altitude" (read: success rate) in this diagram is 24% when combining an insertion angle of 21^0 (indicated by the arrowhead on the x-axis) with an insertion point of 0.47AB (indicated by the arrowhead on the y-axis). This maximal success rate is indicated in white in the diagram. This white area represents a small set of combinations of insertion angles and insertion points with minimal differences. The median value of these combinations in the white area is indicated by the plus sign (+).

Similar diagrams are shown for other regions as indicated above these diagrams.

Note that at the levels Th1-Th2, Th2-Th3, Th10-Th11, L2-L3 and L3-L4 several combinations of insertion points and insertion angles result in multiple small regions with the same maximal success rate. In the diagrams, the median of these white areas representing similar success rates are indicated by a plus sign (+). In Table 3, the optimal insertion points and insertion angles at these specific levels are given numerically as this median.